

Supporting Information

New asymmetric tetradentate phenanthroline chelators with pyrazol and amide groups for complexation and solvent extraction of Ln(III)/Am(III)

Haolong Wang^a, Pengyuan Gao^a, Tengfei Cui^a, Dongqi Wang^b, Jinping Liu^c, Hui He^c, Zongyuan Chen^a, Qiang Jin^a, Zhijun Guo^{a,}*

*^a Frontier Science Center for Rare Isotopes; School of Nuclear Science and Technology,
Lanzhou university, Lanzhou 730000, China*

*^b State Key Laboratory of Fine Chemicals, Liaoning Key Laboratory for Catalytic Conversion
of Carbon Resources, School of Chemical Engineering, Dalian University of Technology,
Dalian 116024, China*

^c Radiochemistry Department, China Institute of Atomic Energy, Beijing 102413, China

**Corresponding author. Tel.: +86 931 8913278; fax: +86 931 8913551*

E-mail address: guozhj@lzu.edu.cn (Z. Guo)

Contents

1. Structures of the relevant ligands	3
2. NMR and HRMS data of the ligands.....	4
3. Solvent extraction experiments.....	7
Extraction kinetic	7
Influence of HNO ₃ concentration on SF _{Am/Eu}	7
Dissolution of the ligands in the aqueous phase.....	8
Influence of ligand concentration	10
4. Two-dimensional NMR spectra of L2	11
5. UV-vis spectrophotometric titration	12
6. Crystal Data and structure refinement of Eu(L1)(NO ₃) ₃	13
7. DFT optimized structures	17

1. Structures of the relevant ligands

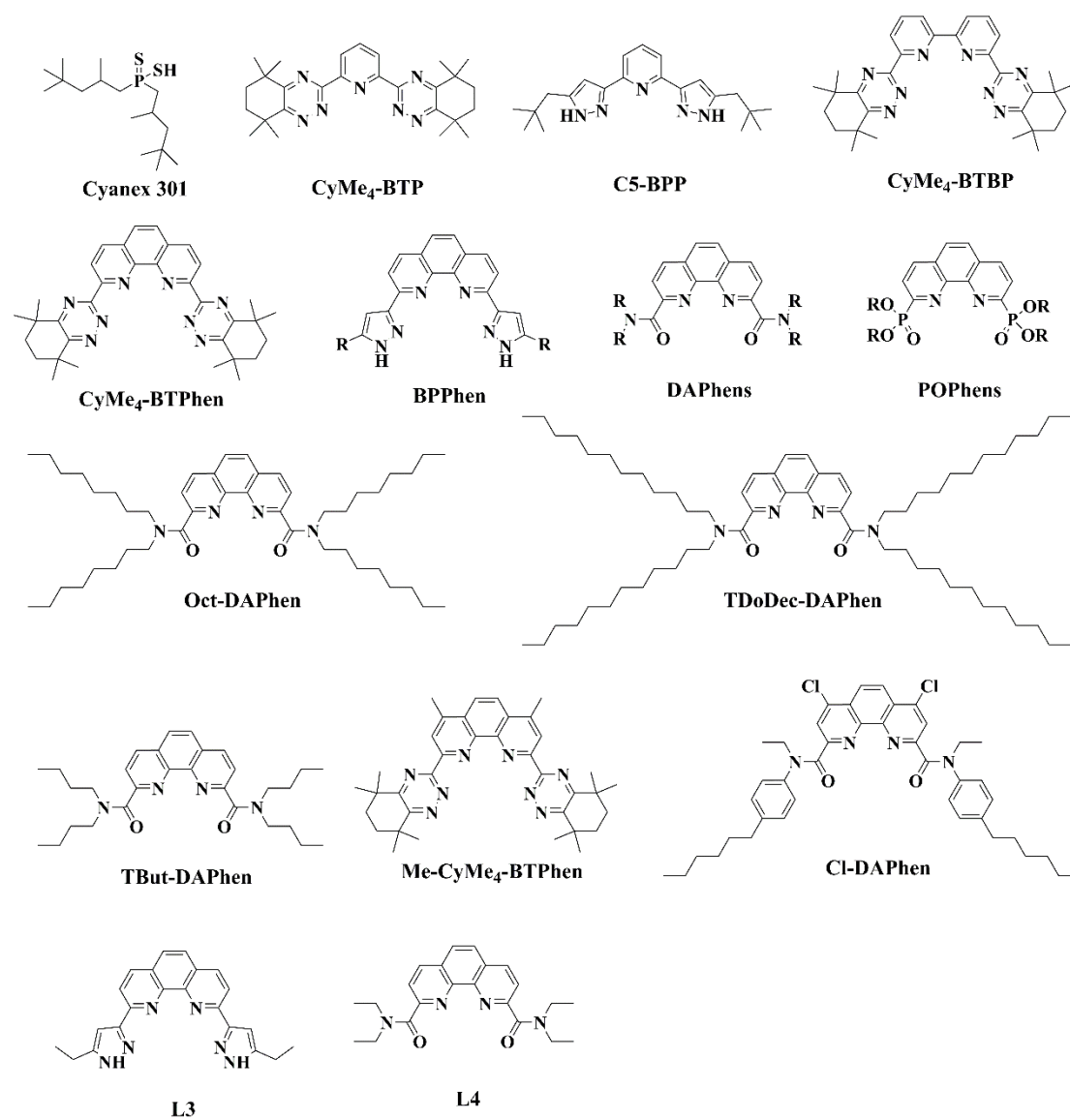


Fig. S1 Structures of the relevant ligands.

2. NMR and HRMS data of the ligands

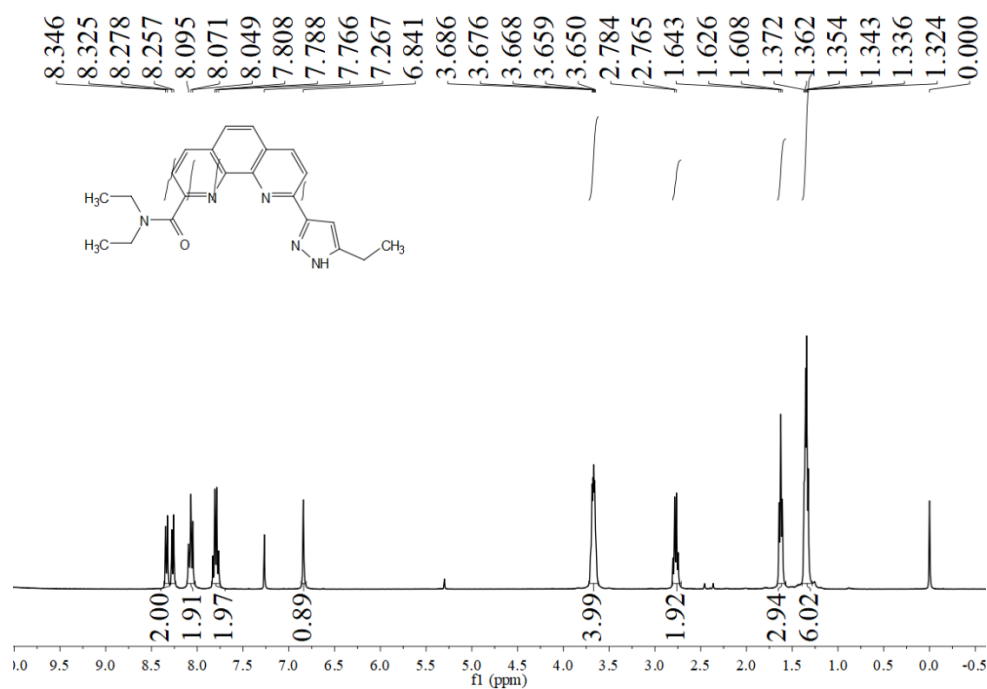


Fig. S2 ^1H NMR spectrum of L1 in CDCl_3 .

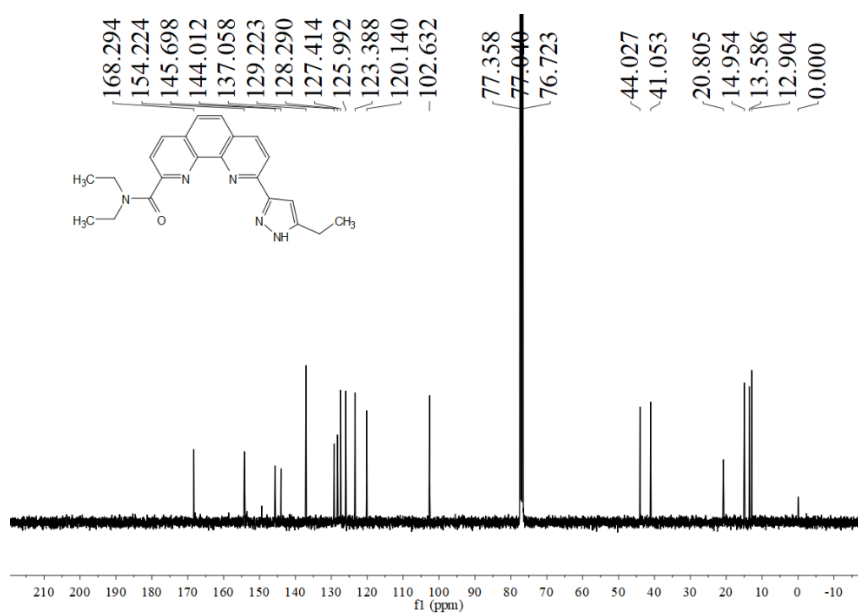


Fig. S3 ^{13}C NMR spectrum of L1 in CDCl_3 .

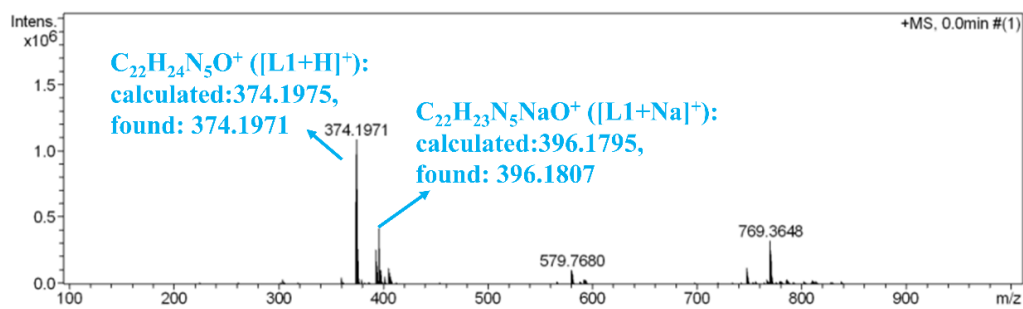


Fig. S4 HRMS (ESI) of L1.

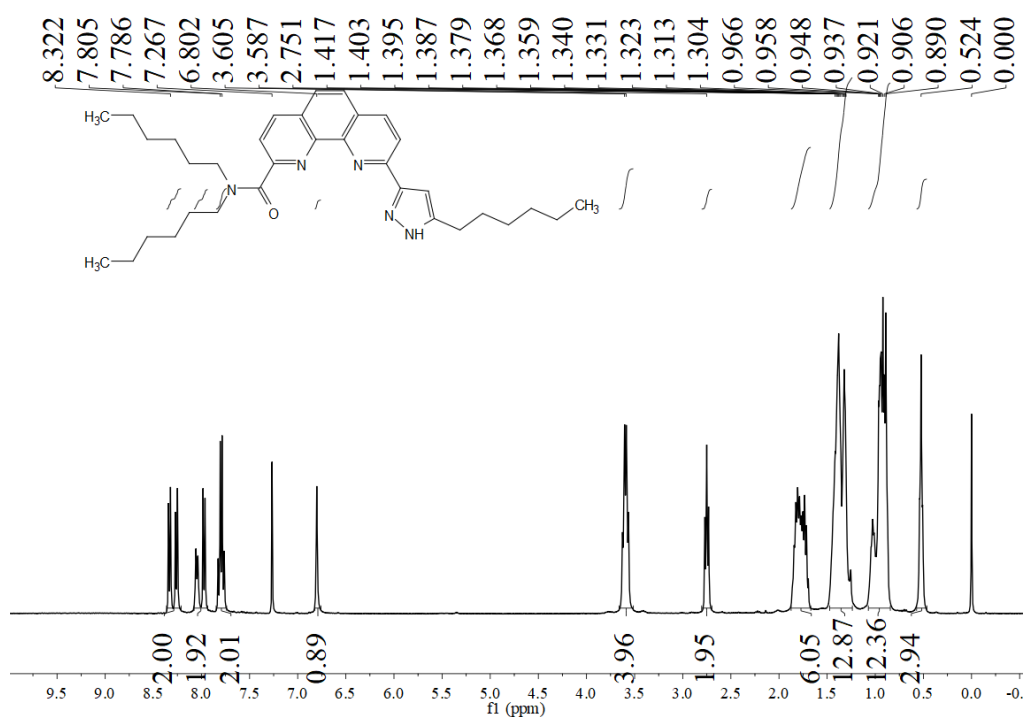


Fig. S5 ¹H NMR spectrum of L2 in CDCl₃.

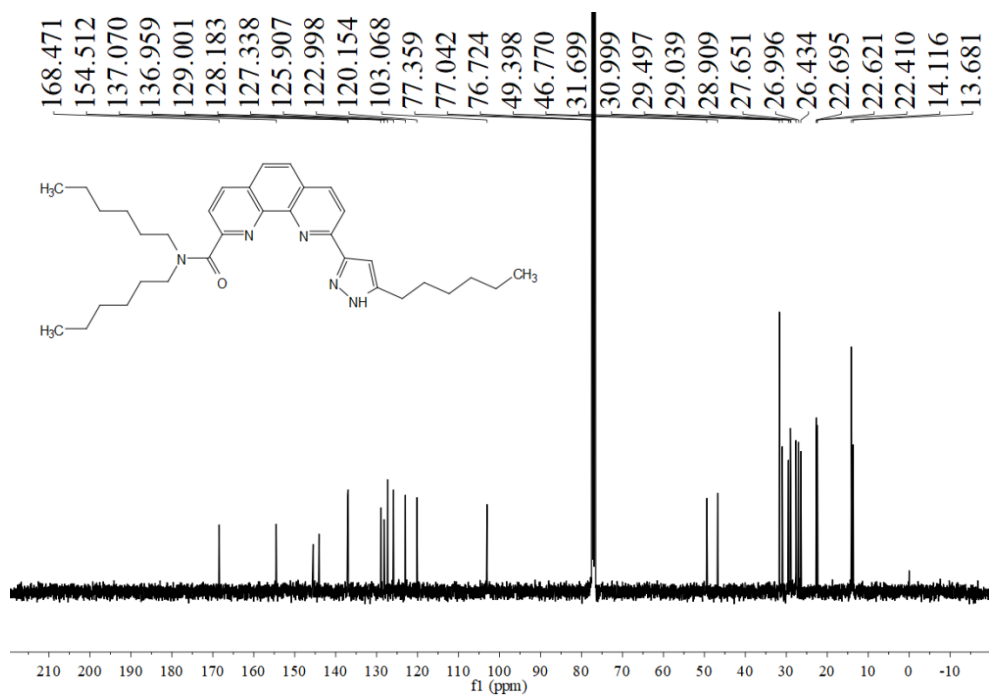


Fig. S6 ¹³C NMR spectrum of L2 in CDCl₃.

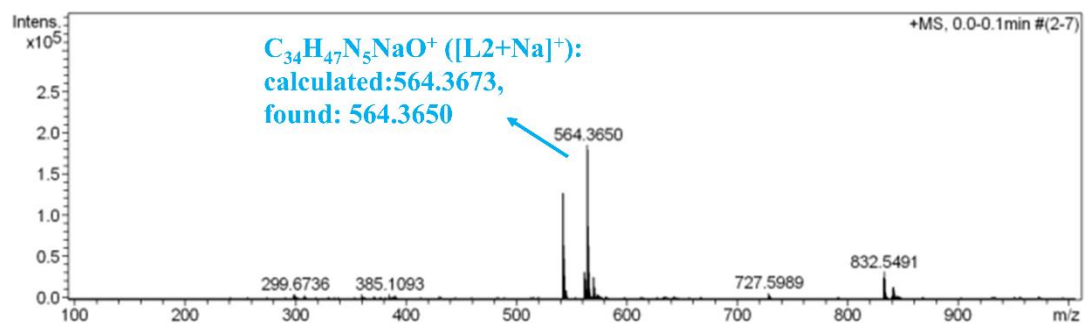


Fig. S7 HRMS (ESI) of L2.

3. Solvent extraction experiments

Extraction kinetic

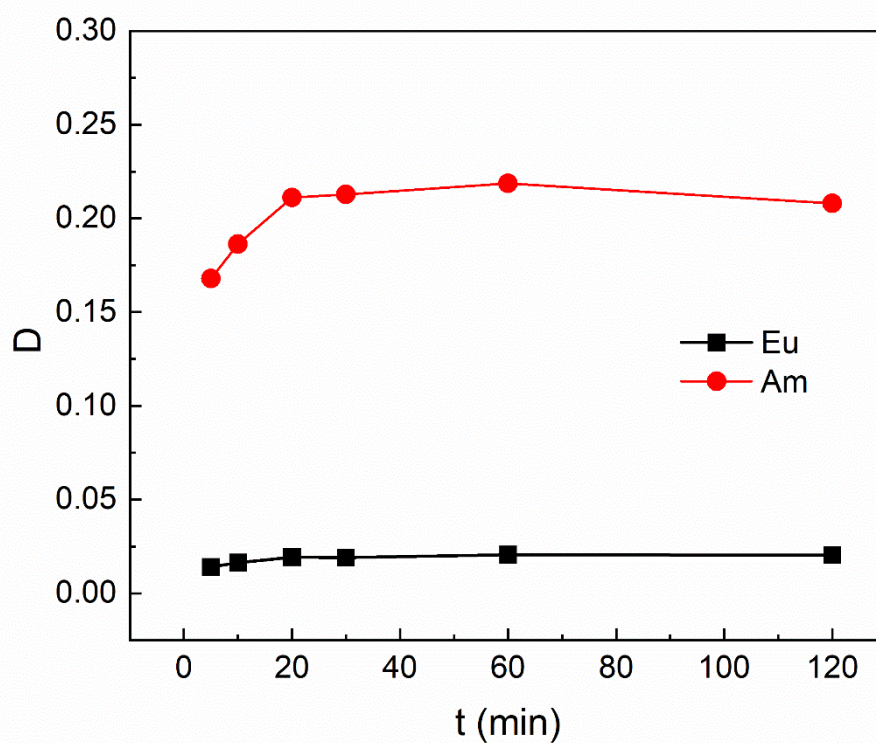


Fig. S8 Influence of contact time on the extraction of Am^{3+} and Eu^{3+} . Organic phase: 0.01 mol/L L2 in 1,2-dichloroethane; Aqueous phase: 1×10^{-4} mol/L $\text{Eu}(\text{NO}_3)_3$ and trace amount of $^{241}\text{Am}/^{152,154}\text{Eu}$ in 3.0 mol/L HNO_3 solution; $T=298$ K.

Influence of HNO_3 concentration on $\text{SF}_{\text{Am/Eu}}$

Table S1 Influence of HNO_3 concentration on $\text{SF}_{\text{Am/Eu}}$ in 1,2-dichloroethane.

HNO_3 , mol/L	L1	L2
0.01	1.9 ± 1.7	1.6 ± 0.8
0.1	1.0 ± 0.4	45.8 ± 5.3
1	15.6 ± 1.5	34.5 ± 2.7

3	6.4±1.3	14.2±1.2
5	1.1±0.7	12.3±1.1

Table S2 SF_{Am/Eu} of relevant ligands.

Ligands	SF _{Am/Eu}	C (HNO ₃) mol/L	Solvent	Lipophilic anion source	References
L2	34.5±2.7	1.0	1,2-Dichloroethane	No	This work
BPPhen	~100	1.0	3-Nitrobenzotrifluoride	2-bromohexanoic acid	1
Et-Tol-DAPhen	67	1.0	Cyclohexanone	No	2
Pyr-DAPhen	~6	1.0	3-Nitrobenzotrifluoride	No	3
Oct-DAPhen	6.5±1.5	3.0	1,2-Dichloroethane	No	4
TButDAPhen	8.9	3;2	3-Nitrobenzotrifluoride	No	5, 6
TDoDecDAPhen	10	3	3-Nitrobenzotrifluoride	No	7
TDoDecDAPhen	6.5	3	Dodecane	No	7

Dissolution of the ligands in the aqueous phase

The dissolution of L1 and L2 was evaluated by contacting L1 and L2 solutions of 1,2-dichloroethane (0.01 mol/L) with the aqueous HCl solutions of different concentrations, respectively. HCl was used instead of HNO₃ owing to the interference of HNO₃ to the absorbance of the ligands at 297 nm. Equal volumes (1.0 mL) of the organic and aqueous phases were stirred in a 3.0 mL vial at 25 °C for 2 h. After phase separation by centrifugation, the concentrations of the ligands in the organic phase were determined directly by the absorbance at 297 nm.

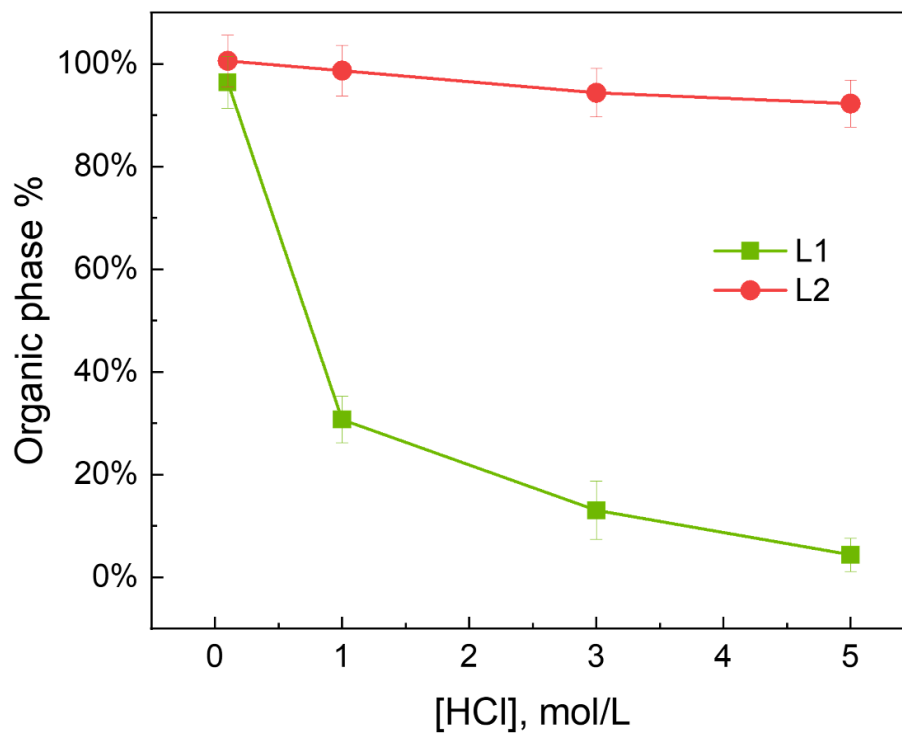


Figure S9. The relative concentration ($C/C_0 \times 100\%$) of the ligands in the organic phase.

$V/V = 1:1$, $C_0 = 0.01$ mol/L.

Influence of ligand concentration

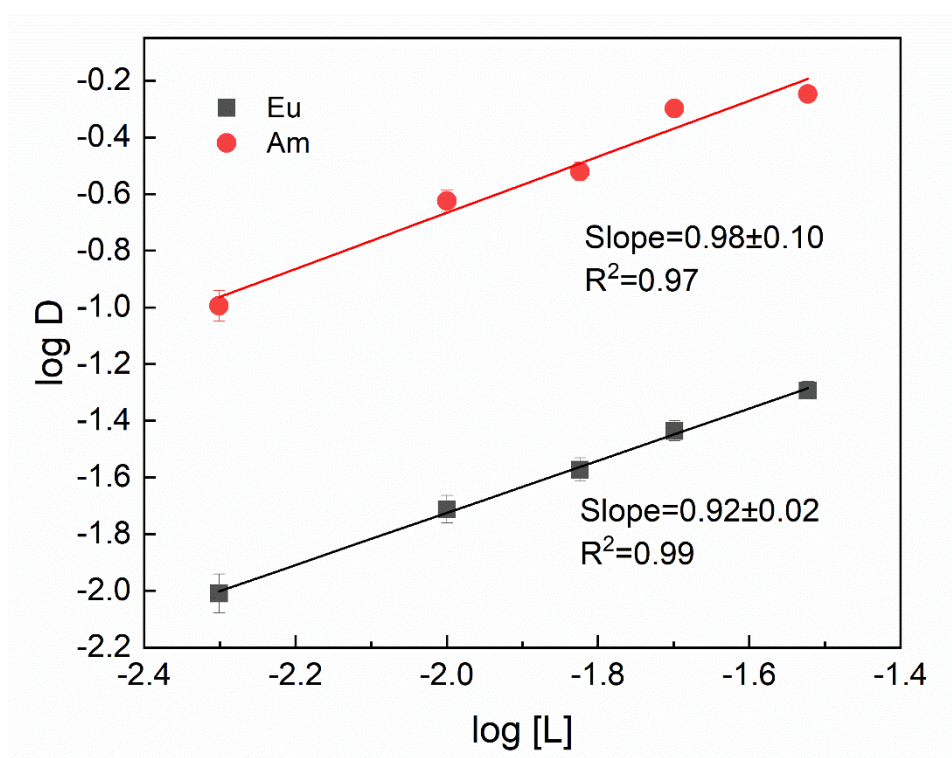


Figure S10. The influence of ligand concentration on the extraction of Am^{3+} and Eu^{3+} . Organic phase: different concentrations of L2 in 1,2-dichloroethane; Aqueous phase: 1×10^{-4} mol/L $\text{Eu}(\text{NO}_3)_3$ and trace amount of $^{241}\text{Am} / ^{152,154}\text{Eu}$ in 3.0 mol/L HNO_3 solution; $T=298$ K.

4. Two-dimensional NMR spectra of L2

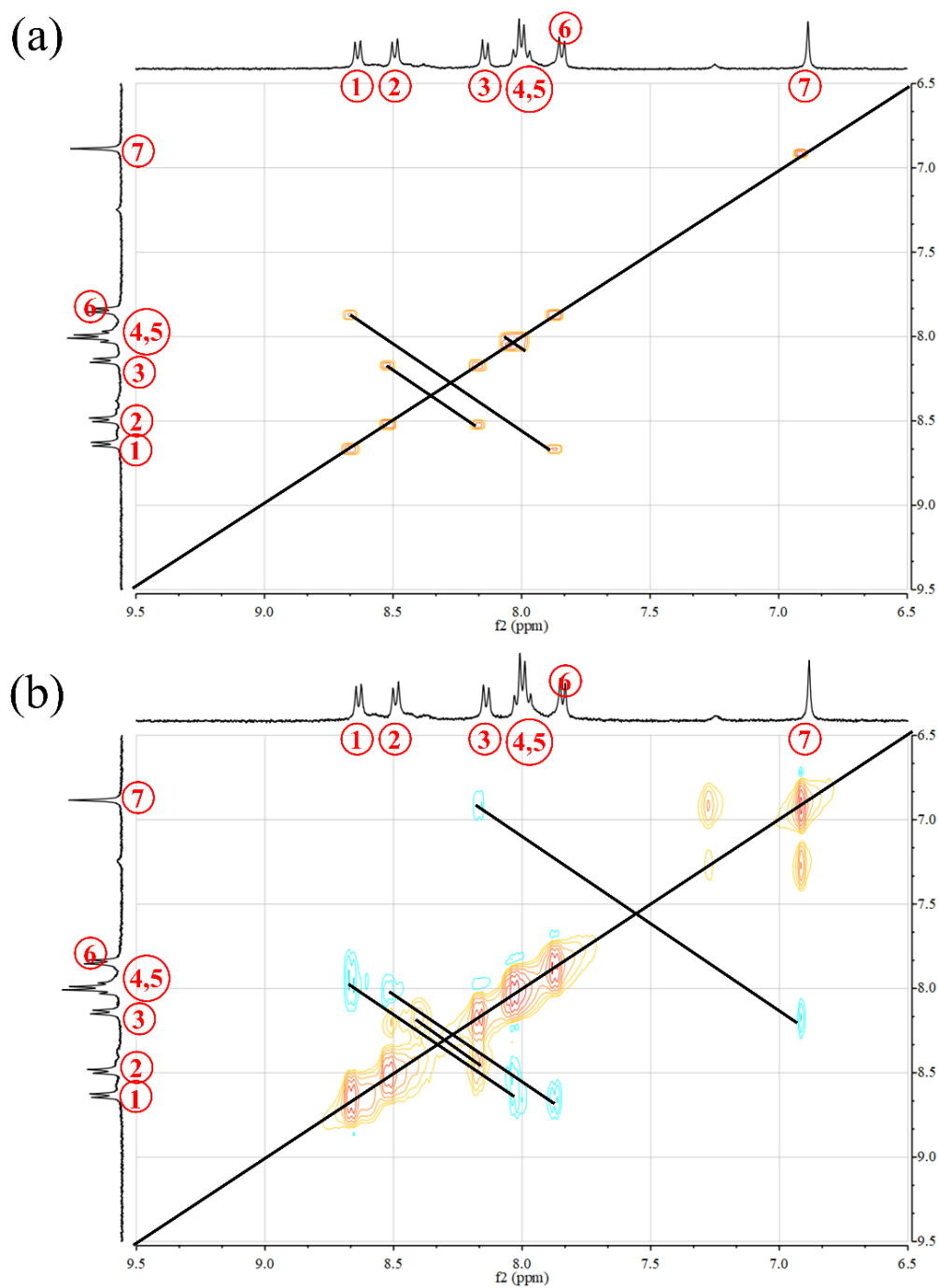


Fig. S11 The ^1H - ^1H COSY and NOESY of L2 in CD_3OD : (a) ^1H - ^1H COSY; (b) ^1H - ^1H NOESY.

5. UV-vis spectrophotometric titration

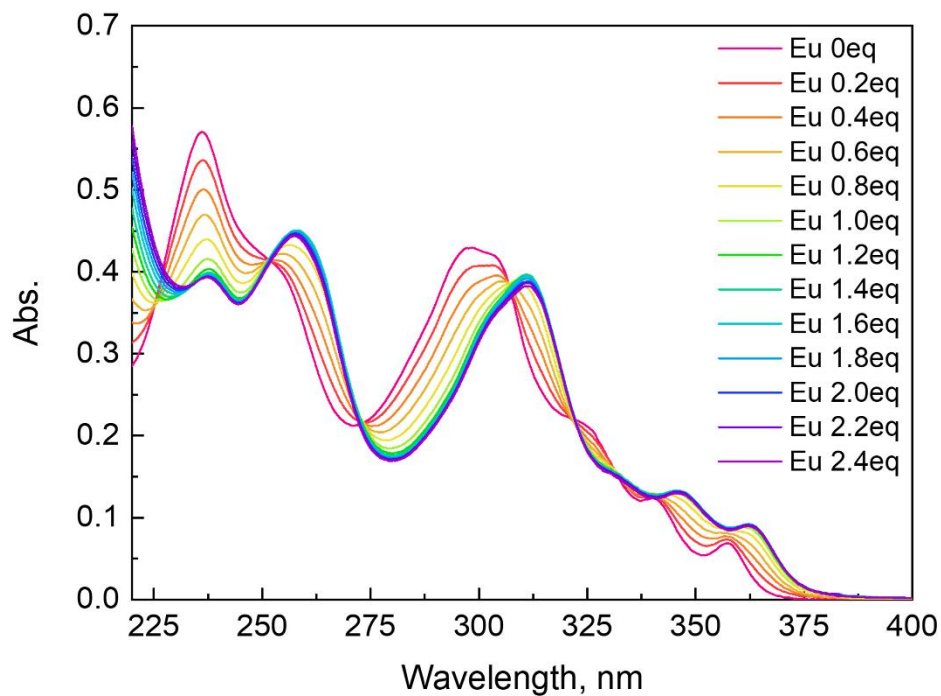


Fig. S12 UV-vis spectrophotometric titration of L1 with Eu³⁺ in methanol at 298 K.

6. Crystal Data and structure refinement of Eu(L1)(NO₃)₃

Table S3 Crystal Data and structure refinement of Eu(L1)(NO₃)₃.

	[Eu(L1)(NO ₃) ₃]
CCDC No.	2130928
Empirical formula	C ₂₂ H ₂₂ EuN ₈ O ₁₀
Formula weight	710.43
Temperature/K	301.74(10)
Crystal system	monoclinic
Space group	P21/n
a/Å	9.1272(3)
b/Å	14.1154(4)
c/Å	20.6307(7)
α/°	90
β/°	95.093(3)
γ/°	90
Volume/Å ³	2647.44(14)
Z	4
ρ _{calc} /cm ³	1.782
μ/mm ⁻¹	2.44
F(000)	1412
Crystal size/mm ³	0.12 × 0.08 × 0.07
Radiation	MoKα (λ = 0.71073)
2θ range for data collection/°	3.5 to 61.874
Index ranges	-12 ≤ h ≤ 11, -19 ≤ k ≤ 16, -25 ≤ l ≤ 25
Reflections collected	19329
Independent reflections	6680 [R _{int} = 0.0335, R _{sigma} = 0.0373]
Data/restraints/parameters	6680/0/373
Goodness-of-fit on F ²	1.018
Final R indexes [I >= 2σ (I)]	R ₁ = 0.0282, wR ₂ = 0.0652
Final R indexes [all data]	R ₁ = 0.0409, wR ₂ = 0.0708
Largest diff. peak/hole / e Å ⁻³	0.88/-0.56

Table S4 Bond lengths of Eu(L1)(NO₃)₃.

Atom	Atom	Length/Å	Atom	Atom	Length/Å
Eu1	O1	2.390(2)	N5	C14	1.325(4)
Eu1	O3	2.637(2)	N5	C17	1.482(4)
Eu1	O4	2.485(2)	N6	N8	1.347(4)
Eu1	O5	2.481(2)	N6	C18	1.355(4)
Eu1	O6	2.481(2)	N8	C4	1.336(3)
Eu1	O8	2.499(2)	C1	C14	1.520(4)
Eu1	O10	2.518(2)	C1	C16	1.397(4)
Eu1	N1	2.643(2)	C2	C19	1.509(5)
Eu1	N4	2.572(2)	C3	C7	1.366(5)
Eu1	N8	2.546(3)	C3	C20	1.402(5)
O1	C14	1.250(4)	C4	C6	1.461(4)
O2	N3	1.214(3)	C4	C10	1.397(4)
O3	N3	1.244(4)	C5	C17	1.503(6)
O4	N2	1.260(4)	C6	C7	1.404(4)
O5	N3	1.272(3)	C8	C12	1.444(4)
O6	N2	1.262(4)	C8	C20	1.407(4)
O7	N7	1.220(4)	C9	C18	1.485(5)
O8	N7	1.254(3)	C9	C21	1.531(7)
O9	N2	1.209(4)	C10	C18	1.386(5)
O10	N7	1.270(4)	C11	C16	1.370(4)
N1	C6	1.332(4)	C11	C22	1.400(5)
N1	C8	1.349(4)	C12	C22	1.402(4)
N4	C1	1.326(4)	C13	C15	1.344(5)
N4	C12	1.352(3)	C13	C22	1.442(4)
N5	C2	1.476(4)	C15	C20	1.426(4)

Table S5 Bond angles of compound Eu(L1)(NO₃)₃.

Atom	Atom	Atom	Angle/°	Atom	Atom	Atom	Angle/°
O1	Eu1	O3	71.85(7)	N7	O10	Eu1	95.62(17)
O1	Eu1	O4	76.69(8)	C6	N1	Eu1	121.47(19)
O1	Eu1	O5	121.05(7)	C6	N1	C8	118.1(2)
O1	Eu1	O6	80.81(8)	C8	N1	Eu1	120.38(18)
O1	Eu1	O8	73.15(7)	O4	N2	Eu1	58.18(15)
O1	Eu1	O10	118.37(8)	O4	N2	O6	115.9(3)
O1	Eu1	N1	120.01(7)	O6	N2	Eu1	58.01(15)
O1	Eu1	N2	76.06(8)	O9	N2	Eu1	174.2(3)
O1	Eu1	N4	62.53(7)	O9	N2	O4	121.6(3)
O1	Eu1	N7	95.52(8)	O9	N2	O6	122.5(3)
O1	Eu1	N8	155.07(8)	O2	N3	Eu1	173.4(3)
O3	Eu1	N1	167.66(8)	O2	N3	O3	123.0(3)
O3	Eu1	N2	91.32(8)	O2	N3	O5	120.9(3)
O3	Eu1	N7	86.66(8)	O3	N3	Eu1	61.64(15)
O4	Eu1	O3	115.06(8)	O3	N3	O5	116.1(3)
O4	Eu1	O8	146.22(8)	O5	N3	Eu1	54.65(14)
O4	Eu1	O10	140.69(8)	C1	N4	Eu1	118.32(18)
O4	Eu1	N1	73.22(8)	C1	N4	C12	118.8(3)
O4	Eu1	N2	25.53(8)	C12	N4	Eu1	122.84(19)
O4	Eu1	N4	79.70(7)	C2	N5	C17	115.2(3)
O4	Eu1	N7	152.25(8)	C14	N5	C2	126.8(3)
O4	Eu1	N8	80.54(9)	C14	N5	C17	117.2(3)
O5	Eu1	O3	49.20(7)	N8	N6	C18	112.6(2)
O5	Eu1	O4	124.21(8)	O7	N7	Eu1	178.6(3)
O5	Eu1	O6	78.24(8)	O7	N7	O8	120.9(3)
O5	Eu1	O8	85.03(9)	O7	N7	O10	122.4(3)
O5	Eu1	O10	81.18(9)	O8	N7	Eu1	57.89(15)
O5	Eu1	N1	118.85(7)	O8	N7	O10	116.7(3)
O5	Eu1	N2	102.08(9)	O10	N7	Eu1	58.82(15)
O5	Eu1	N4	155.97(8)	N6	N8	Eu1	128.46(18)
O5	Eu1	N7	82.79(9)	C4	N8	Eu1	123.5(2)
O5	Eu1	N8	65.16(8)	C4	N8	N6	105.0(2)
O6	Eu1	O3	68.69(8)	N4	C1	C14	111.4(3)
O6	Eu1	O4	50.99(7)	N4	C1	C16	121.9(3)
O6	Eu1	O8	135.49(8)	C16	C1	C14	126.2(3)
O6	Eu1	O10	157.36(9)	N5	C2	C19	113.9(3)
O6	Eu1	N1	114.69(8)	C7	C3	C20	120.1(3)
O6	Eu1	N2	25.55(8)	N8	C4	C6	117.0(3)
O6	Eu1	N4	124.59(8)	N8	C4	C10	111.1(3)
O6	Eu1	N7	155.06(8)	C10	C4	C6	131.6(3)
O6	Eu1	N8	77.01(9)	N1	C6	C4	115.1(2)

O8	Eu1	O3	69.15(8)	N1	C6	C7	122.2(3)
O8	Eu1	O10	50.71(7)	C7	C6	C4	122.6(3)
O8	Eu1	N1	109.55(7)	C3	C7	C6	119.4(3)
O8	Eu1	N2	147.39(8)	N1	C8	C12	117.1(2)
O8	Eu1	N4	73.17(8)	N1	C8	C20	123.7(3)
O8	Eu1	N7	25.15(7)	C20	C8	C12	119.1(3)
O8	Eu1	N8	131.39(8)	C18	C9	C21	109.4(4)
O10	Eu1	O3	104.25(8)	C18	C10	C4	105.4(3)
O10	Eu1	N1	67.89(8)	C16	C11	C22	119.7(3)
O10	Eu1	N2	161.28(8)	N4	C12	C8	117.3(3)
O10	Eu1	N4	77.25(8)	N4	C12	C22	123.0(3)
O10	Eu1	N7	25.56(7)	C22	C12	C8	119.5(3)
O10	Eu1	N8	85.88(9)	C15	C13	C22	120.7(3)
N1	Eu1	N2	94.93(8)	O1	C14	Eu1	39.55(13)
N1	Eu1	N7	88.62(8)	O1	C14	N5	121.6(3)
N2	Eu1	N7	171.54(9)	O1	C14	C1	115.6(2)
N4	Eu1	O3	127.14(8)	N5	C14	Eu1	146.4(2)
N4	Eu1	N1	61.82(7)	N5	C14	C1	122.7(3)
N4	Eu1	N2	101.75(8)	C1	C14	Eu1	83.80(16)
N4	Eu1	N7	73.18(8)	C13	C15	C20	121.2(3)
N8	Eu1	O3	109.69(8)	C11	C16	C1	119.6(3)
N8	Eu1	N1	61.35(8)	N5	C17	C5	112.8(3)
N8	Eu1	N2	79.02(9)	N6	C18	C9	121.6(3)
N8	Eu1	N4	123.00(8)	N6	C18	C10	105.8(3)
N8	Eu1	N7	109.39(9)	C10	C18	C9	132.3(3)
C14	O1	Eu1	121.00(18)	C3	C20	C8	116.5(3)
N3	O3	Eu1	93.83(16)	C3	C20	C15	123.6(3)
N2	O4	Eu1	96.29(18)	C8	C20	C15	119.9(3)
N3	O5	Eu1	100.63(18)	C11	C22	C12	116.9(3)
N2	O6	Eu1	96.44(18)	C11	C22	C13	123.5(3)
N7	O8	Eu1	96.95(17)	C12	C22	C13	119.5(3)

7. DFT optimized structures

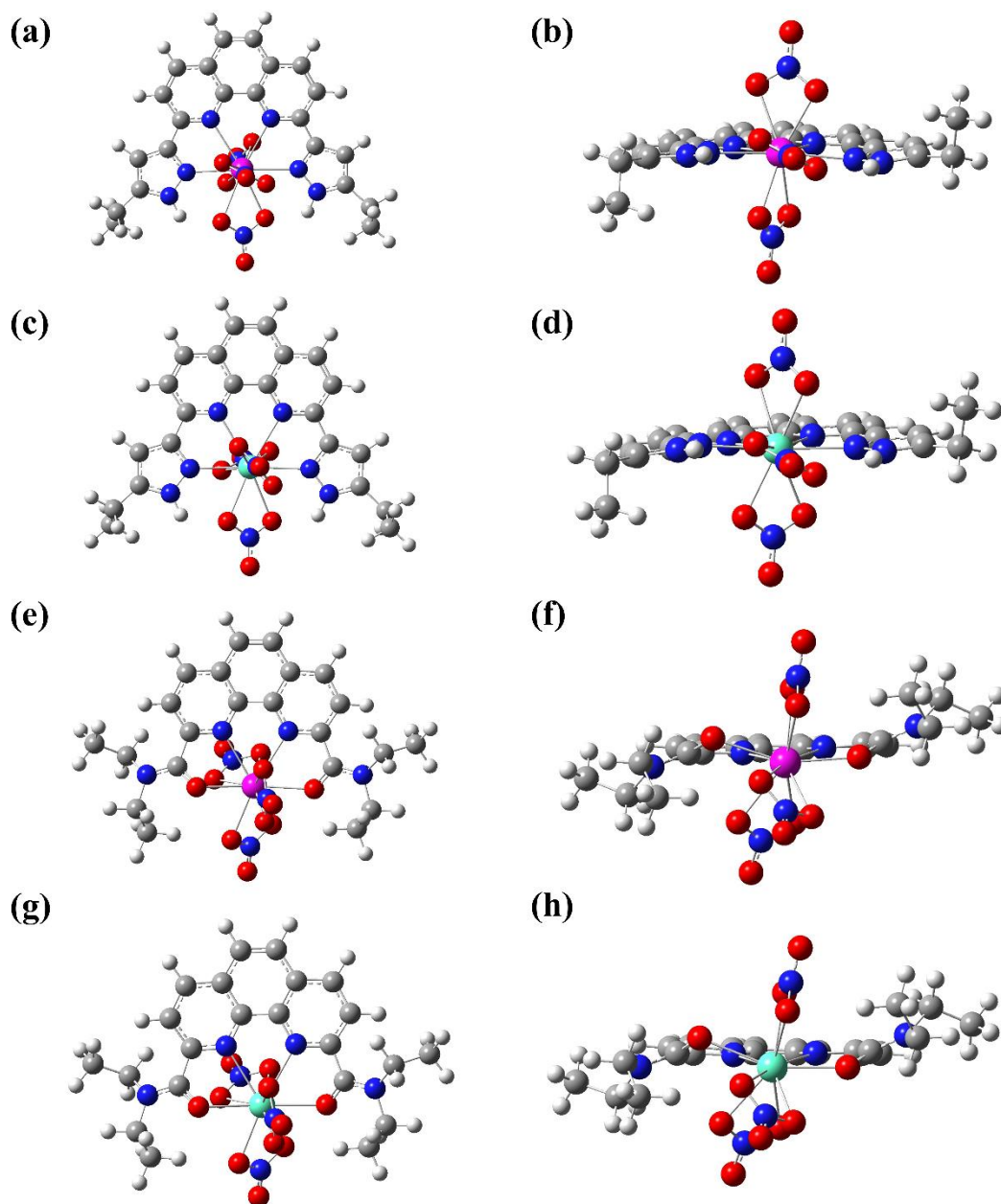


Fig. S13 DFT optimized structures of Am/Eu complexes: (a) Am(L3)(NO₃)₃ top view, (b) Am(L3)(NO₃)₃ side view, (c) Eu(L3)(NO₃)₃ top view, (d) Eu(L3)(NO₃)₃ side view, (e) Am(L4)(NO₃)₃ top view, (f) Am(L4)(NO₃)₃ side view, (g) Eu(L4)(NO₃)₃ top view, (h) Eu(L4)(NO₃)₃ side view. Am: purple, Eu: cyan, C: gray, H: gray white, N: blue, O: red.

References

- 1 Y. Liu, X. Yang, S. Ding, Z. Wang, L. Zhang, L. Song, Z. Chen and X. Wang, Highly Efficient Trivalent Americium/Europium Separation by Phenanthroline-Derived Bis(pyrazole) Ligands, *Inorg. Chem.*, 2018, **57**, 5782-5790.
- 2 C.-L. Xiao, C.-Z. Wang, L.-Y. Yuan, B. Li, H. He, S. Wang, Y.-L. Zhao, Z.-F. Chai and W.-Q. Shi, Excellent Selectivity for Actinides with a Tetradentate 2,9-Diamide-1,10-Phenanthroline Ligand in Highly Acidic Solution: A Hard–Soft Donor Combined Strategy, *Inorg. Chem.*, 2014, **53**, 1712-1720.
- 3 R. Meng, L. Xu, X. Yang, M. Sun, C. Xu, N. E. Borisova, X. Zhang, L. Lei and C. Xiao, Influence of a N-Heterocyclic Core on the Binding Capability of N,O-Hybrid Diamide Ligands toward Trivalent Lanthanides and Actinides, *Inorg. Chem.*, 2021, **60**, 8754-8764.
- 4 S. Jansone-Popova, A. S. Ivanov, V. S. Bryantsev, F. V. Sloop, R. Custelcean, I. Popovs, M. M. Dekarske and B. A. Moyer, Bis-lactam-1,10-phenanthroline (BLPhen), a New Type of Preorganized Mixed N,O-Donor Ligand That Separates Am(III) over Eu(III) with Exceptionally High Efficiency, *Inorg. Chem.*, 2017, **56**, 5911-5917.
- 5 M. Alyapyshev, J. Ashina, D. Dar'in, E. Kenf, D. Kirsanov, L. Tkachenko, A. Legin, G. Starova and V. Babain, 1,10-Phenanthroline-2,9-dicarboxamides as Ligands for Separation and Sensing of Hazardous Metals, *RSC Advances*, 2016, **6**, 68642-68652.
- 6 M. Alyapyshev, V. Babain, L. Tkachenko, E. Kenf, I. Voronaev, D. Dar'in, P. Matveev, V. Petrov, S. Kalmykov and Y. Ustynyuk, Extraction of actinides with heterocyclic dicarboxamides, *J. Radioanal. Nucl. Chem.*, 2018, **316**, 419-428.
- 7 N. Tsutsui, Y. Ban, H. Suzuki, M. Nakase, S. Ito, Y. Inaba, T. Matsumura and K. Takeshita, Effects of Diluents on the Separation of Minor Actinides from Lanthanides with Tetradodecyl-1,10-phenanthroline-2,9-diamide from Nitric Acid Medium, *Anal. Sci.*, 2020, **36**, 241-245.